DE GRUYTER OPEN

Archives of Hydro-Engineering and Environmental Mechanics
Vol. 65 (2018), No. 3, pp. 163–176
DOI: 10.1515/heem-2018-0011

Case-Study Modelling Analysis of Hydrodynamics in the Nearshore of the Baltic Sea Forced by Extreme Along-shore Wind in the Case of a Cross-shore Obstacle *

Andrei Sokolov[1,2], **Boris Chubarenko**[1]

[1] Shirshov Institute of Oceanology, Russian Academy of Sciences, Moscow, Nahimovskiy prospekt 36, Russia, 117997

[2] Immanuel Kant Baltic Federal University, A. Nevskogo 14, Kaliningrad, Russia, 236016,
e-mails: ansokolov@kantiana.ru (corresponding author), chuboris@mail.ru

(Received October 04, 2018; revised December 18, 2018)

Abstract

In the current study we use a three-dimensional model with hydrodynamic and spectral wave modules operating in a coupled mode to simulate the response of currents and wind wave fields to winds of 20–25 m/sec offshore of the protective structure of the Saint Petersburg Flood Prevention Facility Complex. The model was calibrated against field data, which allowed us to obtain a tool describing storm situations in the eastern part of the Gulf of Finland with a satisfactory accuracy. The numerical modeling showed that the protective dam did not have a noticeable effect on the levels of storm surge, significant wave height, or current speed in areas seaward of the dam. The increase in erosion processes on the southern shore of the easternmost part of the Gulf of Finland in recent past has most probably been related to other factors. We found that if a west or south-west wind of at least 25 m/s blows over the Baltic Sea for at least 16 hours, the level of storm surges seaward of the dam may reach 3 or more meters. An artificial strengthening of the coastline and the creation of shore protection structures are recommended.

Key words: numerical modeling, extreme weather, storm surge, wind waves, currents, protective dam, Gulf of Finland

1. Introduction

The "north capital" of Russia, the City of Saint Petersburg, is known for its floods. The rising sea level, in combination with wind waves and currents, has been a dangerous factor for embankments, buildings, and bridges over the past hundreds of years. Since the foundation of the city in 1703, there have been 3 truly catastrophic flood events: on September 21, 1777 the water level rose by 321 cm; on November 19, 1824 it rose by 421 cm; and on September 23, 1924 it rose by 380 cm (Ryabchuk et al 2011).

* This paper is dedicated to the memory of Professor Zbigniew Pruszak (1947–2018).

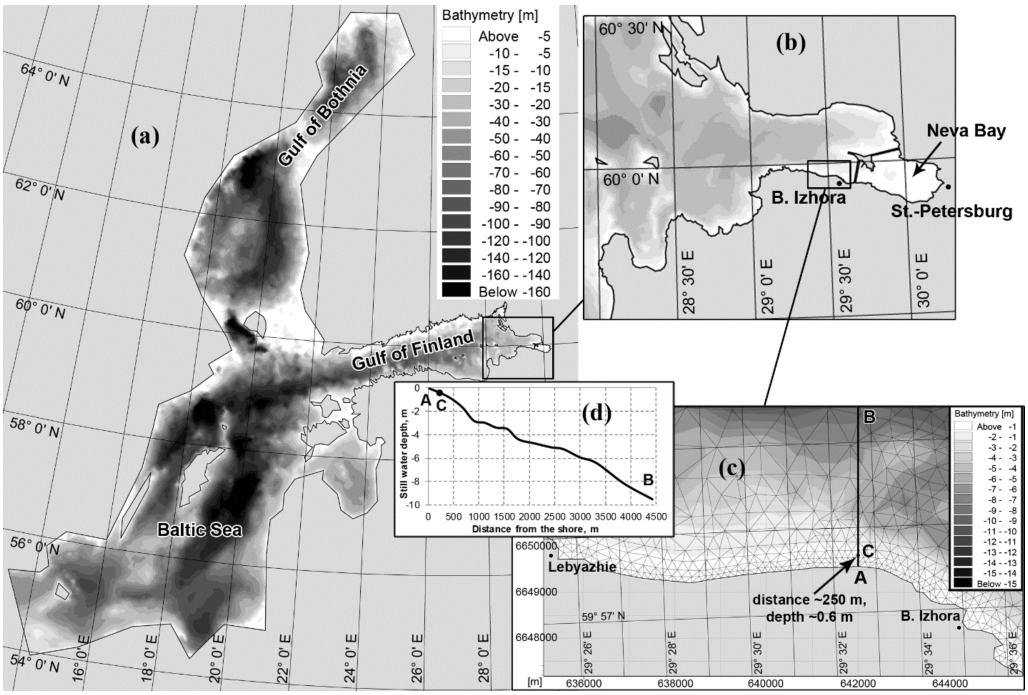

Fig. 1. (a) – the computational domain with a bathymetric map; (b) – the eastern part of the Gulf of Finland; the Neva Bay is bounded by a protective dam; (c) – the study area in detail with a numerical grid. The control point C is marked by an arrow. The AB profile will be used for presentation of the main results; the depth profile is presented in panel (d)

Considering that tides in the Baltic Sea are only a few centimeters high (Wróblewski 2001), the above water level rises were indeed extreme. Floods in Saint Petersburg are very irregular. There may be several floods within a year, but several years may also pass without flooding (Ryabchuk et al 2011).

According to the orientation of the Gulf of Finland, the prevailing winds from west and southwest can move water from almost the entire Baltic Sea into the eastern part of the gulf (see Fig. 1a). Winds from these directions with speeds higher than 5 m/sec are the most probable (5–8%) in that area (Ryabchuk et al 2011). To protect the city against floods, the construction of the Saint Petersburg Flood Prevention Facility Complex,[1] connecting the northern and southern shores of the Gulf of Finland via the Kotlin Island (Kronstadt), was initiated in 1979. The dam complex, with a total length of 23.4 km, was finished in 2011. It has 6 gates for water movement and 2 passages for ships, also equipped with automatic gates. Since the dam complex separates the Neva Bay from the Gulf of Finland, the bay can be classified as an artificial estuarine lagoon (Ryabchuk et al 2017). The water in the Neva Bay is fresh, as the bay receives the runoff of the main river in the Baltic basin, the Neva River. At the time when the

[1] https://en.wikipedia.org/wiki/Saint_Petersburg_Dam

complex was planned, it was assumed that the dam would not seriously affect water areas located seaward of the dam. The present situation is compared with historical conditions in (Ryabchuk et al 2012, 2016, Kovaleva et al 2014, Leontjev et al 2015).

The aim of the present study was to determine whether the influence of the protective dam on hydrodynamic conditions in its vicinity is essential or not. In other words, what would happen under extreme weather conditions in the presence and absence of the dam? How would the maximum surge level change? What would be the significant wave height and the speed of currents during the maximum sea level?

We focused our attention on the nearshore area between the villages of Lebyazhie and B. Izhora, the southern shore of the Gulf of Finland just seaward of the dam (the study area in Fig. 1c). For the past ten years, this area has been attracting considerable attention because of unpredictable and sometimes ruinous coastal erosion (Ryabchuk et al 2017).

The study was limited by the use of numerical modeling only to reveal the effect of the dam's presence, with all other factors considered equal.

2. Method

Numerical modeling was performed using the software package MIKE developed by DHI Software (MIKE 2017a, 2017b). A three-dimensional formulation (5 sigma-coordinate layers in depth) was used for simulations. Two modules (hydrodynamic and spectral wave) were used in a coupled model to resolve a system of differential equations.

2.1. Basic Equations

The *Hydrodynamic Module* solves numerically Navier-Stokes equations in a 3-dimensional shallow water approximation (MIKE 2017a); the simulated variables are the surface elevation (η) and current velocity components in the x, y, and z direction (u, v, and w):

$$\frac{\partial u}{\partial x} + \frac{\partial v}{\partial y} + \frac{\partial w}{\partial z} = 0, \tag{1}$$

$$\begin{aligned} &\frac{\partial u}{\partial t} + \frac{\partial u^2}{\partial x} + \frac{\partial vu}{\partial y} + \frac{\partial wu}{\partial z} = \\ &fv - g\frac{\partial \eta}{\partial x} - \frac{1}{\rho_0}\frac{\partial p_a}{\partial x} - \frac{g}{\rho_0}\int_z^\eta \frac{\partial \rho}{\partial x}dz + F_u + \frac{\partial}{\partial z}\left(v_t \frac{\partial u}{\partial z}\right), \end{aligned} \tag{2}$$

$$\frac{\partial v}{\partial t} + \frac{\partial v^2}{\partial x} + \frac{\partial uv}{\partial y} + \frac{\partial wv}{\partial z} = \\ -fu - g\frac{\partial \eta}{\partial y} - \frac{1}{\rho_0}\frac{\partial p_a}{\partial y} - \frac{g}{\rho_0}\int_z^\eta \frac{\partial \rho}{\partial y}dz + F_v + \frac{\partial}{\partial z}\left(v_t \frac{\partial v}{\partial z}\right), \tag{3}$$

where t is time; x, y, z are the Cartesian coordinates; f is the Coriolis parameter; g is the gravity acceleration; ρ_0 and ρ are a reference value and the deviation of water density, respectively; p_a is the atmospheric pressure; v_t is the vertical turbulent (or eddy) viscosity; F_u and F_v are the horizontal stress terms.

The *Spectral Wave Module* gives a time-dependent 2-dimensional plane (x, y) solution for wind wave variables using the wave action density (N) balance equation (MIKE 2017b):

$$\frac{\partial N}{\partial t} + \frac{\partial}{\partial x}c_x N + \frac{\partial}{\partial y}c_y N + \frac{\partial}{\partial \omega}c_\omega N + \frac{\partial}{\partial \theta}c_\theta N = \frac{S}{\omega}, \tag{4}$$

where θ is the wave direction; ω is the relative (intrinsic) angular frequency; and c_x, c_y, c_ω, and c_θ are propagation velocities in x-, y-, ω-, and θ-space, respectively.

According to the equation, the total change of action density in the control volume (due to the local rate of change of action density in time, its advection in geographical space, shifting of the relative frequency due to variations in depths and currents, depth-induced and current-induced refractions) is balanced by the energy source term (S), which represents the superposition of source functions:

$$S = S_{in} + S_{nl} + S_{ds} + S_{bot} + S_{surf}. \tag{5}$$

The following sources are included in the model: S_{in} – the generation of energy by wind, S_{nl} – wave energy transfer caused by non-linear wave-wave interaction, S_{ds}, S_{bot}, S_{surf} – wave energy dissipation due to whitecapping, bottom friction, and depth-induced breaking, respectively.

2.2. Numerical Model Set-up

The computational domain covered almost the entire Baltic Sea area, about 1000 km from west to east and about 1300 km from north to south (Fig. 1). The depth field was taken from the digital topography of the Baltic Sea (Seifert, Kayser 1995). The mesh sizes of an irregular grid were about 5–10 km for the open sea, and about 100 m in the vicinity of the area of interest. In total, the model has 5 sigma-coordinate layers in depth. All boundaries of the computational domain were closed, and wind was the only driving force in the model. Low wind conditions are rarely uniform over the entire Baltic Sea. However, as claimed by (Cerkowniak et al 2015), extreme storm impacts on the Baltic shores are due mostly to waves generated by persistent wind fields, which are approximately homogeneous over the entire basin. Therefore, it

was assumed that wind was uniform in speed and direction over the entire simulation area (Soomery 2001). The above model setup showed (Sokolov, Chubarenko 2018) its advantages for coupled hydrodynamic and wind-wave simulations near the shore and was proposed for the first time in (Sokolov, Chubarenko 2012).

The influence of the Neva River was not taken into account, as we focused on simulating hydrodynamic conditions on the seaward side of the dam under extreme weather conditions, when the gates of the dam complex are closed.

A fully spectral formulation was used for simulations of wind waves. Frequency discretization parameters were chosen in order to cover waves from the shortest wind waves to the swell. The following set of parameters allowed us to resolve waves with periods from 0.8 to 14 seconds with a reasonable accuracy:

- discretization type: logarithmic;
- minimum frequency: 0.07 Hz (the longest wave period is about 14 s);
- frequency factor: 1.1;
- number of frequencies: 30 (the shortest wave period is about 0.8 s).

Preliminary simulations showed that the main parameter affecting the duration of the CPU workload was the directional discretization. Ultimately, a 24-direction spatial discretization was found optimal, as the use of more directions had almost no effect on the result, but required much more computational time. For a smaller number of directions, the differencies in the wave fields obtained were quite noticeble.

The other main parameters for the spectral wave module were taken as follows:

- a coupled type of air-sea interaction with a background Charnock parameter of 0.01 (Brown and Wolf 2009);
- nonlinear quadruplet-wave interaction is included;
- wave breaking is included with dimensionless parameters $\alpha = 1$ and $\gamma = 0.8$ (Allard et al 2002);
- sand grain size of 0.25 mm for the bottom friction model.

2.3. Calibration of the Model

The calibration of the hydrodynamic module (Sokolov, Chubarenko 2018) was based on field data collected by the Institute of Hydro-Engineering of the Polish Academy of Sciences (IBW PAN) in the vicinity of the Lubiatowo Field Station (South-Eastern Baltic) between October 1 and November 22, 2006 (Pruszak et al 2008): the speed of currents at ordinates from 0.4 m to 2.4 m above the bottom were measured by an ADCP located 200 meters from the shoreline at a depth of 4–4.4 m, depending on water level variations; the wind data were provided by an automated meteorological station. The first results of the calibration and verification of the model setup for depth-averaged currents were presented in (Sokolov, Chubarenko 2012).

The spectral wave module was also calibrated with respect to the IBW PAN field data (Pruszak et al 2008). These data were recorded by a wave buoy (Directional

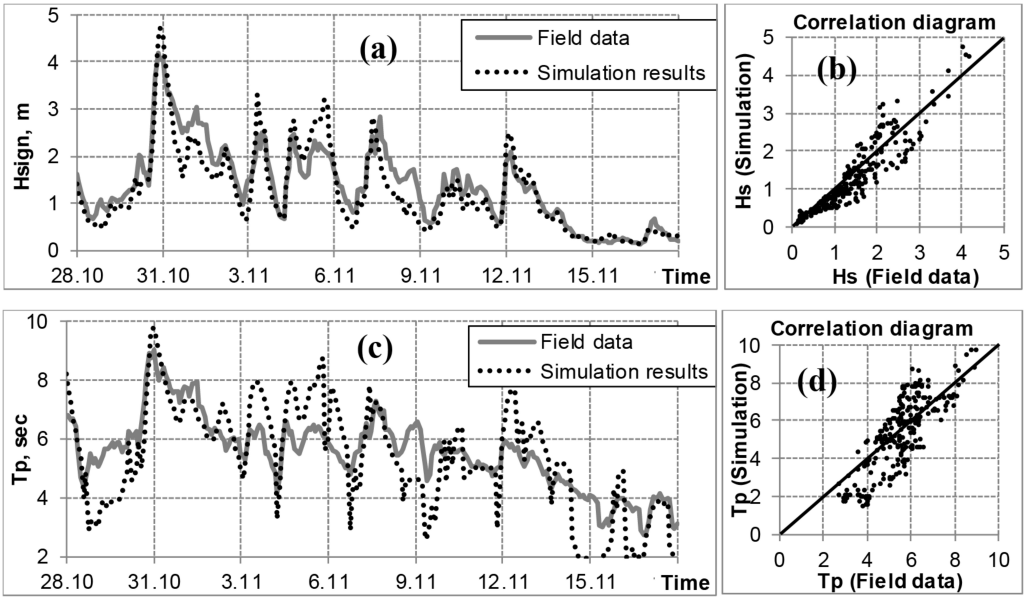

Fig. 2. Field measurement data and simulation results ($C_{dis} = 7$) for the significant wave height H_s (a, b), and the peak wave period T_p (c, d) for the period of 28 Oct.–18 Nov. 2006

Waverider) between October 23 and November 18, 2006. The buoy was installed about 2 kilometers from the shore at a depth of 15 m. The main calibration parameter of the model should be the white-capping dissipation coefficient, whose optimal value was found to be $C_{dis} = 7$.

The time of appearance and magnitude of peaks provided by field measurements and model simulations (Fig. 2) are similar. The average difference between significant wave heights does not exceed 0.13 m, and the maximum difference is about 1 m. The average difference between wave peak periods is about 0.2 second, and the maximum difference is about 3 seconds. The satisfactory similarity between the field and model data is illustrated by statistics in Table 1, following (Roland et al 2009).

The negative bias indicates that the model underestimates the significant wave height and period, and the relative discrepancy is less than 10%. The root mean square error (RMSE) is higher than the bias. It means that the error of the model solution at any given moment of time is greater than the error averaged over time. The relative error is about 22–27%, as shown by the Scatter Index. Correlation coefficients (the possible maximum is 1) for the wave height and period are rather high, but the model solution for the wave height is better than for the wave period.

The calibration results demonstrate that the model setup takes into account basic factors needed for the calculation of both wave fields and current fields in the nearshore with sufficient accuracy. The model solution for $C_{dis} = 7$ was found optimal, as it gave the best results for individual values (relative errors for wave height and period were the lowest, in the range of 21–22%), while the relative discrepancy of this

Table 1. Statistical comparison of the field and simulation data for wave heights and peak periods for different values of the white-capping dissipation coefficient (C_{dis}). The bias (the difference between the mean of simulations and observations) shows how the model solution represents real characteristics on average. The root mean square error (RMSE) means the same and it applies to an individual item in time series of measured and modelled characteristics. The Scatter Index (RMSE normalized by the mean measured value (Statistics 2014)) shows the relative error of the modeling solution with respect to measurements. The correlation coefficient shows the level of synchronicity between variations in measured and modeled characteristics

No	Parameter	$C_{dis} = 5$		$C_{dis} = 7$		$C_{dis} = 9$	
		Hs	Tp	Hs	Tp	Hs	Tp
1.	Mean of the observations	1.36 m	5.54 s	1.36 m	5.54 s	1.36 m	5.54 s
2.	Mean of the simulations	1.4 m	5.62 s	1.24 m	5.33 s	1.12 m	5.14 s
3.	Bias = (2) – (1)	0.04 m	0.08 s	−0.12 m	−0.21 s	−0.24 m	−0.4 s
4.	Relative bias = (3) / (1)	2.9%	1.4%	−8.8%	−3.8%	−17.6%	−7.2%
5.	RMSE	0.46 m	1.24 s	0.37 m	1.2 s	0.39 m	1.21 s
6.	Scatter Index = (5) / (1)	34%	22%	27%	22%	29%	22%
7.	Correlation coefficient	0.91	0.79	0.92	0.79	0.93	0.79

model solution for values averaged over the whole period is not the least possible. The solution for $C_{dis} = 5$, on average, describes the measured time series better (relative biases are 2.9% and 1.4% for wave height and period, respectively).

2.4. Simulation Scenarios

The preliminary simulations showed that the highest sea level and the significant wave height near the study area are observed when the wind blows from west-southwest. Therefore, this direction (247.5 degrees) was selected for further modeling aimed at analyzing extreme hydrodynamic conditions.

The forcing scenario of extreme conditions included a step-wise wind action following calm initial conditions. The wind was uniform in speed and direction throughout the computational area, as the size of intensive cyclones is greater than the area of the Baltic Sea (Soomere 2001). Two wind speeds were considered: 20 or 25 m/sec.

To understand the influence of the dam complex on hydrodynamic parameters, the simulations were performed in the domain with and without the dam. These variations gave a total of 4 simulation scenarios. The hydrodynamic parameters were recorded for the eastern part of the Gulf of Finland, along the AB profile (see Fig. 1c) and at a control point located about 250 m seaward of the coastline.

3. Results

3.1. Levels of Storm Surges

The numerical solution for the water level after a step-wise wind action demonstrates that the Baltic Sea seeks equilibrium (Fig. 3). In the example of the control point C (250 m offshore at a depth of 0.6 m, under calm initial conditions, marked by an

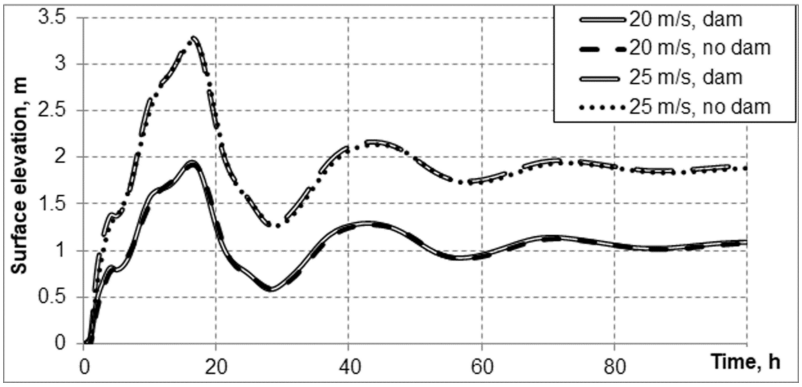

Fig. 3. Levels of storm surges (surface elevation) against time for west-southwest winds (247.5 degrees, 20 and 25 m/s) in simulations with and without the dam

arrow in Fig. 1c), we can see that time-dependent variations in water level are damped oscillations with an approximate period of 28 hours. It takes about 3 days to reach the steady state solution for wind surge (surface elevation in the model terminology). For winds of 20 and 25 m/s, the wind surge is estimated at 1.1 and 1.85 m, respectively, so the actual depth at the control point becomes 2–3 times greater than the initial one for calm conditions.

According to the simulations of scenarios with and without the dam, the wind surge for winds of 20 and 25 m/s is nearly identical, as the maximum differences do not exceed 5 cm. The highest rise in surge level occurs at the first peak, and its value depends on the wind speed, but the period of oscillation does not depend on the wind speed (Table 2). In both cases, the first peak happened 16.5 hours after wind had started and it was 70–80% higher than the steady state solution. The second peak was 18% higher than the steady state solution.

Table 2. The height and time of the maximum possible water level rise for west-southwest winds (247.5 degrees) of 20 and 25 m/s in the simulations with and without the dam

Wind speed	With the dam		Without the dam	
	Max. level [m]	Time [h]	Max. level [m]	Time [h]
20 m/sec	1.94	16.5	1.91	16.5
25 m/sec	3.28	16.5	3.23	16.5

3.2. Wave Impact

Once the water level variations in time are principally identical in all scenarios, we compare wave parameters at the moment when the wind surge is maximal (the first peak in Fig. 3) and, therefore, waves are most developed.

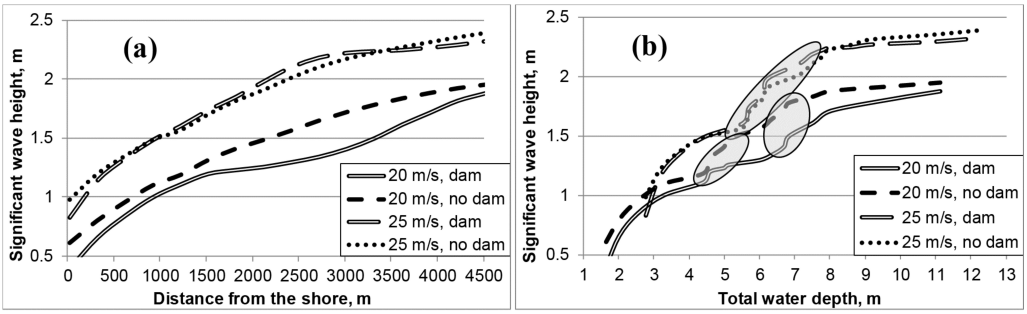

Fig. 4. Significant wave height along the AB profile for WSW winds of 20 and 25 m/s against the distance from the shore (a) and the total water depth (b) when the storm surge is the highest. The total water depth means still water depth plus surface elevation (storm surge) – it is nearly 3 m at point C for the wind of 25 m/s. Zones of wave breaking are marked by shadowed ellipses

The cross-shore profiles (Fig. 4, along the AB line) of the significant wave height for a wind speed of 25 m/s with and without the dam are almost identical. If the wind speed is 20 m/s, the significant wave height in the presence of the dam is even lower than it is without the dam, and the difference is noticeable (0.2–0.3 m).

Fig. 4b clearly illustrates nearshore wave dynamics. We can see zones of wave breaking. For a WSW wind of 20 m/sec, two zones are visible, when the total water depth (depth with a storm surge) is about 7 m and 5 m. For a wind of 25 m/sec, there is a single wide zone from a depth of 5.5 to 7.5 m.

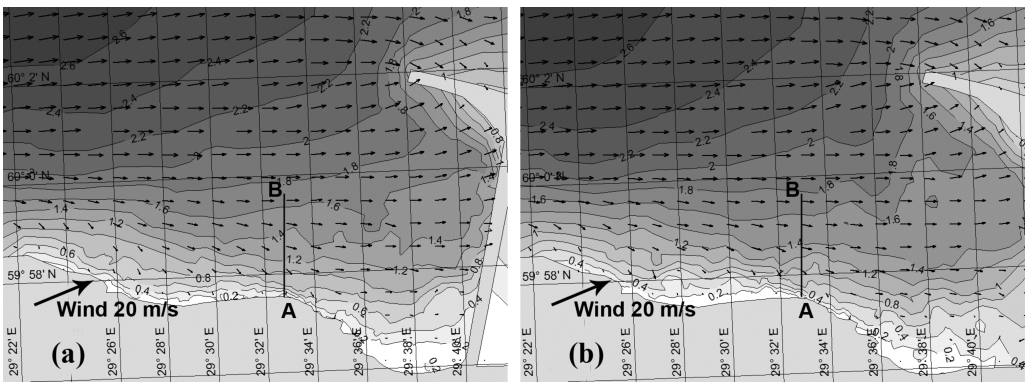

Fig. 5. Wave fields under a WSW wind of 20 m/s: (a) with the dam, (b) without the dam. Arrows indicate directions of wave propagation, isolines show the significant wave height

Fig. 5 shows wave fields (a) with the dam and (b) without it for a WSW wind of 20 m/s. We cannot see any significant differences in the study area. The wave height obviously decreases toward the east because of decreasing water depth, and the dam does not affect this process. Fig. 6 illustrates wave fields with the dam under winds of 20 m/s from other directions (W, NW, N, NE). Wind fields are very similar for all winds from the western quarter (WNW, W, NW) – the wave heights are determined

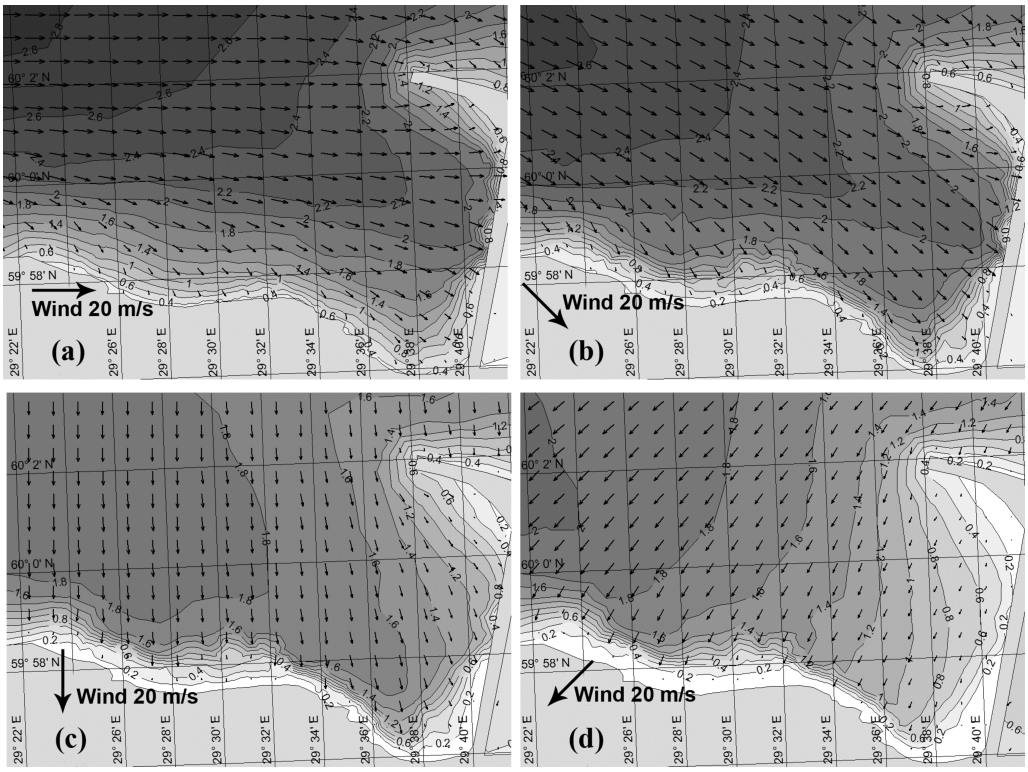

Fig. 6. Wave fields under winds of 20 m/s from (a) W, (b) NW, (c) N, (d) NE: Arrows indicate directions of wave propagation, isolines show the significant wave height. The dam is present

by wind fetch and the water depth decreasing toward the Neva Bay (along the Gulf of Finland). For N and NE winds, the wind fetch is much (several times) smaller, but waves develop until their heights are only several percent smaller than those for western winds.

3.3. Near-bottom Currents

Typical current fields in the bottom layer with and without the dam are shown in Fig. 7. The events with the highest water level rise have been chosen. The dam is the non-transparent obstacle in the way of the current passing over the southern shore, and it reflects this current toward the north (Fig. 7a). It is necessary to emphasize that, in the absence of the dam, the anticyclonic vortex to the south of the Kotlin Island (Fig. 7b) remains, but diminishes in size.

The current speed in the bottom layer at the control point C is 3–5 cm/s less in the presence of the dam. The simulated values are 35–40 cm/s when the wind speed is 20 m/s, and 50–55 cm/s when the wind speed is 25 m/s.

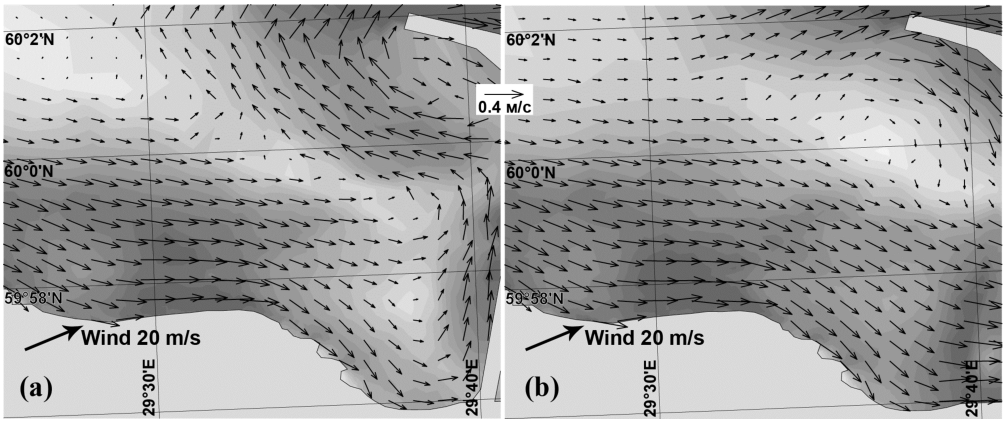

Fig. 7. Current fields in the bottom layer: (a) with the dam, (b) without the dam. Wind of 20 m/s from WSW (247.5 degrees). Currents are given at the moment when the sea level rise is maximal

4. Discussion

The simulation results suggest that the construction of the dam has affected hydrodynamic conditions in the study area. As a result of the dam, the levels of storm surges have increased by no more than 5 cm. Moreover the influence of the dam appears to be positive for a number of parameters. When the dam was absent, the water level was increased not only by storm surges, but also by waters of the Neva River. In the model setup, the Neva River is absent, which slightly decreases the water level without the dam. With the construction of the dam, the significant wave height remained almost unchanged, or even decreased by 20–30 cm in the depth interval of 5–7 m. The speed of bottom currents also remained almost unchanged or decreased by 3–5 cm/s. In our opinion, such slight changes in hydrodynamic parameters may not absolutely exclude the negative effect of the dam on the southern shore of the easternmost part of the Gulf of Finland, but they cast a doubt on its dominant role in erosion processes.

Factors that can lead to erosion of the coastline may be divided into 4 groups: meteorological, morphological, anthropogenic, and climatic. The main meteorological factors are wind waves, storm surges, and ice cover. The most intensive erosion occurs in fall and winter, when three components coincide: a significant sea level rise, stormy winds from west or south-west, and the absence of ice cover (Ryabchuk et al 2011). This intensive erosion event is not a periodic one – an extreme storm can destroy the coastline after several "calm" years with a stable coastline.

From the perspective of morphological dynamics, the most important factors are coastline orientation and the properties of the coastal slope. The coastline in the study area is oriented from west to east and is relatively straight. Thus, this area is almost open to wave actions during storms from west and north-west.

With regard to anthropogenic factors, the dam is not the only such factor that can potentially lead to erosion. Another one is the Londonskaya Otmel mine, which is an

active underwater sand mine located near the study area. It is also worth mentioning that a number of engineering structures and houses have been built on the shore disregarding the tendencies of evolution of the coastal zone. The main climatic factor that can lead to an increase in erosion is the rise of the sea level. This factor seems to be important in most climate scenarios.

It should be noted that the greatest level of storm surge obtained in the simulations both in the absence and in the presence of the dam is 3.5 m (for a WSW wind of 25 m/s blowing over the whole Baltic Sea for at least 16 hours). It is clearly understandable that under such wind conditions the southern shore will be flooded. Although the water level increase is not likely to reach 3.5 m, since the flood zone would absorb a lot of water, the consequences could be catastrophic.

It can be noticed in the wave-distance and wave-depth profiles (Fig. 5) that the height of the waves decreases stepwise as they approach the shore along the AB profile. At the shore of the South-East Baltic (e.g. the northern shore of the Sambia Peninsula) (Sokolov, Chubarenko 2014), the wave height decrease is rather sharp and clearly visible in the wave breaking zone. In the case of the southern shore of the easternmost part of the Gulf of Finland, there are two not very evident wave breaks and a step-like decrease in wave height in between. This situation can probably be explained by the fact that the underwater slope in the eastern part of the Gulf of Finland is very flat. For example, the slope of the bottom along the AB profile is about 0.002, hence the angle of inclination is slightly greater than 0.1 degree. In contrast, for the northern shore of the Sambia Peninsula, this indicator is 3–4 times greater (slope of the bottom is 0.005–0.008).

Judging from the very small angle of the bottom slope and the fact that the eastern part of the Gulf of Finland is very shallow, even at a large distance from the shore, it seems probable that long waves coming from the Baltic Sea have numerous breaks along with a large wind fetch and become shorter. Consequently, the wave action on the coastline does not appear to be strongly dependent on the size of the area over the Baltic Sea, where the wind speed and direction can be considered uniform.

Comparing the wave fields with and without the dam (Fig. 6), we cannot see any differences that could lead to catastrophic erosion in the study area. This may be explained by the fact that we used a statistical spectral wave model in the present simulations. Perhaps it would be useful to perform simulations using a model that is more accurate in a restricted area, such as a Boussinesq model.

The modeled speed of near-bottom currents 200 m seaward of the shore was 35–40 cm/s for a wind of 20 m/s and 50–55 cm/s for a wind of 25 m/s. These values do not exceed typical values for nearshore areas, for example, in the South-East Baltic (Babakov 2010). The structure of currents changed, of course, when the dam had been built, but near the study area these changes seem insignificant (see Fig. 7). In our opinion, changes in the structure and parameters of currents caused by the dam cannot lead to the intensive erosion processes observed in that area.

5. Conclusions

1. The results of numerical modeling showed that the protective dam does not have a significant effect on the levels of storm surge, significant wave height, or current speed in nearshore areas seaward of the dam. The increase in erosion processes on the southern shore of the easternmost part of the Gulf of Finland over the past years has most probably been related to other factors.
2. It was found that if a west or south-west wind of at least 25 m/s blows over the Baltic Sea for at least 16 hours, the level of storm surges seaward of the dam may reach 3 m or more. This can be catastrophic for the surrounding area.
3. An artificial strengthening of the coastline (preferably by artificial beaches) and the creation of wave protection structures are recommended.

Acknowledgments

Authors thank Dr. Darya Ryabchuk (Karpinski Geological Institute, Saint Petersburg, Russia) for initiating this study and colleagues from the Department of Coastal Engineering and Dynamics of the Institute of Hydroengineering of the Polish Academy of Sciences (Gdañsk, Poland) for providing wave measurement data for calibration of the model. The model setup and wave model verification was supported by project 18-05-80035 of the Russian Fund for Basic Researches, and the analysis was performed with support of theme No 0149-2018-0012/0149-2019-0013 of the State Assignment of IO RAS. The authors appreciate Prof. Rafaş Ostrowski's valuable comments and suggestions, which were very helpful in improving the manuscript.

References

Allard R., Rogers E., Carroll S. N., Rushing K. V. (2002) *Software Design Description for the Simulating Waves Nearshore Model (SWAN)*, pp. 219.

Babakov A. (2010) Wind-driven currents and their impact on the Morpho-lithology at the eastern shore of the Gulf of Gdansk, *Archives of Hydro-Engineering and Environmental Mechanics*, **57** (2), 85–103.

Brown J. M., Wolf J. (2009) Coupled wave and surge modelling for the eastern Irish Sea and implications for model wind-stress, *Continental Shelf Research*, **29**, 1329–1342.

Cerkowniak G., Ostrowski R., Szmytkiewicz P. (2015) Climate change related increase of storminess near Hel Peninsula, Gulf of Gdañsk, Poland, *Journal of Water and Climate Change*, **6** (2), 300–312.

Kovaleva O., Ryabchuk D., Sergeev A., Zhamoida V., Nesterova E. (2014) Abrazionnie processi yuzhnoi beregovoi zoni Finskogo zaliva: prichini, dinamica, prognoz razvitiya. [Erosion processes at the south shore of the Gulf of Finland: causes, dynamics, forecast of development], *Scientific Transactions of the Russian State Hydrometeorological University*, No 35, 87–101 (in Russian).

Leontjev I., Ryabchuk D., Sergeev A., Kovaleva O. (2015) Prognoz recessii beregov vostochnoi chasti Finskogo zaliva na blizhaishee stoletie. [A projection of the recession of the eastern part of the Gulf of Finland in the nearest century], *Oceanology*, **55** (3), 480–487 (in Russian).

MIKE (2017a) *MIKE 21 and MIKE 3 Flow Model FM. Hydrodynamic module: Short description*, DHI software, DHI Water and Environment, Horsholm, 14, https://www.mikepoweredby-dhi.com/-/media/shared%20content/mike%20by%20dhi/flyers%20and%20pdf/product-documentation/short%20descriptions/mike213_fm_hd_short_description.pdf (last call 12.11.2017).

MIKE (2017b) *MIKE 21 wave modelling with MIKE 21 SW (Spectral wave module FM): Short description*, DHI Software, DHI Water and Environment, Horsholm, 16, https://www.mikepoweredby-dhi.com/-/media/shared%20content/mike%20by%20dhi/flyers%20and%20pdf/product-documentation/short%20descriptions/mike21_sw_fm_short_description.pdf (last call 12.11.2017).

Pruszak S., Szmytkiewicz P., Ostrowski R., Skaja M., Szmytkiewicz M. (2008) Shallow-water wave energy dissipation in a multi-bar coastal zone, *Oceanologia*, **50** (1), 43–58.

Roland A., Cucco A., Ferrarin C., Hsu T.-W., Liau J.-M., Ou S.-H., Umgiesser G., Zanke U. (2009) On the development and verification of a 2-D coupled wave-current model on unstructured meshes, *Journal of Marine Systems*, **78**, 244–254.

Ryabchuk D., Kolesov A., Chubarenko B., Spiridonov M., Kurennoy D., Soomere T. (2011) Coastal erosion processes in the eastern Gulf of Finland and their links with geological and hydrometeorological factors, *Boreal Env. Res*, **16** (suppl. A), 117–137.

Ryabchuk D., Spiridonov M., Zhamoida V., Nesterova E., Sergeev A. (2012) Long term and short term coastal line changes of the Eastern Gulf of Finland. Problems of coastal erosion, *Journal of Coastal Conservation*, **16**, Issue 3, 233–242.

Ryabchuk D., Sergeev A., Kovaleva O., Leontjev I., Zhamoida V., Kolesov A. (2016) Problemi abrazii beregov vostochnoi chasti Finskogo zaliva: sostoyanie, prognoz, rekomendacii po beregozachite. [Problems of erosion of the south shore of the Gulf of Finland: present condition, forecast, recommendation for coastal protection], *Scientific Transactions of the Russian State Hydrometeorological University*, **44**, 187–203 (in Russian).

Ryabchuk D., Zhamoida V., Orlova M., Sergeev A., Biblichenko J. Biblichenko A., Sukhacheva L. (2017) Neva Bay: a technogenic lagoon of the Eastern Gulf of Finland (Baltic Sea), [in:] *The Diversity of Russian Estuaries and Lagoons Exposed to Human Influence, Estuaries of the World*, Kosjan R. (ed.), Springer International Publishing, Switzerland, 191–221.

Seifert T., Kayser B. (1995) A high resolution spherical grid topography of the Baltic Sea, *Meereswissenschaftliche Berichte*, **9**, 72–88.

Sokolov A. N, Chubarenko B. V. (2012) Wind influence on the formation of nearshore currents in the Southern Baltic: numerical modelling results, *Archives of Hydroengineering and Environmental Mechanics*, **59** (1–2), 37–48.

Sokolov A. N, Chubarenko B. V. (2014) Analiz vozmozhnogo vliyaniya klimaticheskih izmenenij na parametri vetrvogo volneniya v pribrezhnoi zone iugo-vostochnoi Baltiki [Sensitivity analysis for the wave regime in the wave-deformation zone in the South-Eastern Baltic in view of possible climate changes], *KSTU NEWS*, **34**, 43–51 (in Russian).

Sokolov A., Chubarenko B. (2018) Numerical simulation of dynamics of sediments disposed in the marine coastal zone of South-Eastern Baltic, *Baltica*, **31** (1), 13–23.

Soomere T. (2001) Extreme wind speeds and spatially uniform wind events in the Baltic Proper, *Proc. Estonian Acad. Sci*, **7/3**, 195–211.

Statistics (2014) *Coastal Inlets Research Program (CIRP) Wiki*, Version of 5 June 2014. https://cirpwiki.info/wiki/Statistics.

Wróblewski A. (2001) Lunar nodal tide in the placeBaltic Sea, *Oceanologia*, **43** (1), 99–112.